

The effect of FIR emission from SDSS galaxies on the SFD Galactic extinction map

Kazuhiro YAHATA¹, Atsunori YONEHARA¹, Yasushi SUTO¹,
Edwin L. TURNER², Tom BROADHURST³, and Douglas P. FINKBEINER²
¹*Department of Physics, School of Science, The University of Tokyo, Tokyo 113-0033*

²*Princeton University Observatory, Peyton Hall, Princeton, NJ 08544, USA*

³*Department of Astronomy and Astrophysics, Tel-Aviv University, Israel*

yahata@utap.phys.s.u-tokyo.ac.jp

(Received 2006 0; accepted 2006 0)

Abstract

We compare the most successful and widely used map of Galactic dust extinction, provided by Schlegel, Finkbeiner & Davis (1998; hereafter SFD), to the galaxy number counts in the Sloan Digital Sky Survey (SDSS) photometric/spectroscopic DR4 sample. We divide the SDSS survey area into 69 disjoint subregions according to the dust extinction provided by SFD and compare the surface number density of galaxies in each subregion. As expected, the galaxy surface number density decreases with increasing extinction but only for SFD extinction values above about 0.1 to 0.2 magnitudes (depending on the band). At lower values of the SFD extinction, we find that *the sky surface density of galaxies increases with increasing extinction, precisely the opposite of the effect expected from Galactic dust*. We also find that the average color of the SDSS photometric galaxy sample is bluer at higher SFD extinctions in this regime, again the opposite of the effect expected from Galactic dust. Even though these anomalies occur only for sight-lines with low SFD extinction values, they affect over 70% of the high Galactic latitude sky in which galaxies and their clustering properties are normally studied. Although it would be possible to explain these effects with a mysterious component of Galactic dust which is anti-correlated with the $100\mu\text{m}$ flux on which the SFD extinction map is based, this model is not physically plausible. Moreover, we find that the surface number density of SDSS photometric quasars does not show any similar effect, as would be expected if the explanation were an unknown Galactic dust component. Considering these results, we suggest that the far infrared (FIR) brightness of the sky in regions of true low dust extinction is significantly “contaminated” by the FIR emission from background galaxies. We show that such an explanation is both qualitatively and quantitatively consistent with the available data. Based on this interpretation we conclude that

systematic errors in the SFD extinction map due to extragalactic FIR emission are quite small, of order hundredths of a magnitude, but nevertheless statistically detectable. Unfortunately, however, these errors are also entangled in a complex way with a signal of great interest to many “precision cosmology” applications, namely the large scale clustering of galaxies.

Key words: ISM: dust, extinction — cosmology: large-scale structure of universe — cosmology: observations

1. Introduction

Understanding the properties of dust is a fundamental goal in astronomy and cosmology, as is correcting for its effects on other observables. Mapping dust extinction over the sky is crucial to extracting correct astrophysical quantities from observables. In particular it is essential in measuring the large scale structure of the universe. For instance, if one does not properly correct for Galactic dust extinction, the surface number densities of galaxy behind strongly obscured regions are reduced systematically, producing apparent void structures and distorting the real cosmic clustering signal.

For such purposes, Schlegel, Finkbeiner & Davis (1998; hereafter, SFD) constructed a dust extinction map (hereafter, the SFD-map), which has been used very extensively for a wide variety of astronomical and cosmological studies.

The SFD-map was obtained by the following procedures: (i) making dust temperature and emissivity maps (0.7° FWHM spatial resolution) from COBE/DIRBE data at $100\ \mu m$ and $240\ \mu m$. (ii) making a finer resolution map for dust emission ($6.1'$ angular resolution) from IRAS/ISSA data at $100\ \mu m$ using the COBE temperature map as a calibrator. (iii) making final maps of reddening and extinction assuming a simple linear relation between $100\mu m$ flux and dust column density with a temperature correction for dust emissivity.

For most astronomical purposes one wants an “absorption-weighted” dust extinction map. Since extinction in the SFD-map is inferred from dust emission, however, it corresponds to an “emission-weighted” map. Therefore, if the proportionality between reddening and emissivity breaks down in some regions, for example, the SFD-map could be a poor representation of the actual extinction map. And in any case, there is no guarantee that the assumptions on which the SFD-map is based are accurate enough to construct a highly accurate and reliable account of Galactic extinction and reddening. For such reasons, SFD carried out several tests of the derived maps in their initial studies. They found that the SFD-map reproduces intrinsic colors of elliptical galaxies as estimated from the Mg II index (Faber et al. 1989) with an accuracy roughly twice as good as the dust extinction map provided by Burstein and Heiles (1978, 1982) based on HI 21-cm emission. They also found that the SFD-map tends to overestimate

reddening at very high dust column densities. Also, indications of possible systematic errors emerged from considerations of the conversion coefficient between dust emissivity and dust reddening as determined by two different techniques: 1 - removing the correlation between the colors of brightest cluster galaxies and the SFD-map, versus 2 - a comparison of dust emission with galaxy number counts in the APM galaxy survey (SFD). The coefficients determined by these two techniques differ by approximately a factor of two.

In this paper, we evaluate the SFD-map by a comparison with galaxy number counts from the latest SDSS data release. Fukugita et al. (2004) carried out a similar study using the earlier galaxy catalog provided by the Sloan Digital Sky Survey (SDSS:York et al. (2000)), Data Release 1 (DR1;Abazajian et al. (2003)). They found that dust extinction values estimated from the DR1 galaxy counts are in good agreement with the SFD ones. The availability of the latest catalog of SDSS (Data Release 4; Adelman-McCarthy. et al. 2006) allows us to subject the SFD-map to a new and higher precision test.

2. The Data

2.1. The Sloan Digital Sky Survey DR4

The SDSS DR4 covers 6670 deg² of sky area and contains 180 million objects with photometry in five pass bands, u , g , r , i , and z (Fukugita et al. 1996; Gunn et al. 1998; Hogg et al. 2001; Pier et al. 2003; Blanton et al. 2003; Ivezić et al. 2004; Smith et al. 2002; Gunn et al. 2006; Tucker et al. 2006). In the database, each object is catalogued with not only its photometric properties but also the dust extinction estimated from the SFD-map, $A_{x,\text{SFD}}$, ($x=u,g,r,i$ and z). The conversion factor from reddening, $A_{x,\text{SFD}}/E(B-V)$, in the SFD-map to $A_{x,\text{SFD}}$ is provided by SFD (see Table 6 of SFD). To compute these factors, it was assumed that all objects have the spectral energy distribution of an elliptical galaxy and that Galactic dust properties are the same in all directions (as seen from the Earth); in particular, we then adopt the extinction curve parameter:

$$R_V \equiv A_V/E(B-V) = 3.1, \quad (1)$$

(see Stoughton et al. 2002 and Appendix B of SFD).

Figure 1 shows the SDSS DR4 photometric survey area, and r -band SFD-extinction $A_{r,\text{SFD}}$ in the same part of the sky. Figure 2 shows the cumulative area of the regions where the value of $A_{r,\text{SFD}}$ is lower than a certain value $A_{r,\text{SFD,max}}$. We exclude the regions with relatively high extinction, $A_{r,\text{SFD}} > 0.534$, whose total fractional area is less than 0.2%. The gray thin lines indicate the boundary of subregions each containing about 100 deg² of sky (see section 3.1). The region corresponding to $A_{r,\text{SFD}} < 0.1$ is indicated in both figure 1 and figure 2; this is the regime in which an anomalous correlation of the SDSS galaxy counts with the SFD-map is demonstrated in section 3.

2.2. Constructing a Photometric Galaxy Sample

In this paper, we initially assume that after correction for dust extinction, the surface number density of galaxies will be homogeneously averaged over sufficiently large areas of the sky, and that any remaining inhomogeneities indicate an error in the estimated extinction.

For this analysis, accurate star-galaxy separation is important since the spatial distribution of stars is not homogeneous and is likely to be correlated with the dust distribution. We therefore carefully constructed a reliable photometric galaxy sample for our analysis as follows:

1. False objects are discarded using photometric processing flags.
2. Masked regions are excluded.
3. A magnitude range is determined so as to ensure the reliability of the star-galaxy separation procedure.

Details of these three steps are described below.

2.2.1. False objects

First we remove those photometric objects in the database table that have saturated fluxes, were observed during bad sky conditions, or are fast-moving (and thus suspected of being in the Solar System).

While one could also remove objects with interpolated fluxes, we have chosen to retain them because they are preferentially associated with specific bad CCD pixels and, therefore, are not randomly distributed on the sky. In other words, the additional photometric uncertainty associated with pixel defects seems less likely to produce systematic errors in our analysis than excluding a non-random spatial distribution of objects entirely.

2.2.2. Masks

The SDSS database defines masked regions on the basis of five different conditions. Our analysis excludes regions labeled “BLEEDING”, “BRIGHT_STAR”, “TRAIL”, or “HOLE”, but keeps those labeled “SEEING” which occupy a significant fraction of the entire survey area. We ignore the “SEEING” information because the effect of relatively bad seeing is not serious for photometry of bright galaxies. The total area of the masked regions we exclude is about 70 deg^2 , roughly 1% of the overall survey region.

2.2.3. Magnitude range

We select galaxies from those DR4 objects in which the “type” attribute is equal to GALAXY. The resulting number counts of galaxies are plotted in figure 3 as a function of magnitudes *uncorrected* for the SFD-extinction, m_x .

For our current purpose, we would like to construct subsets of the galaxy sample which are not contaminated by mis-identified stars to the extent possible. For this purpose we restrict the range of magnitudes in the analysis below.

Star-galaxy separation is based on the difference between the composite model magnitude and the PSF magnitude (Abazajian et al. 2004). The reliability of this separation procedure depends on the magnitude of objects (Yasuda et al. 2001; Scranton et al. 2002; Strauss et al. 2002). In the r -band, the procedure is known to be reliable down to ~ 21 mag. The saturation of stellar images typically occurs for $m_r < 15$. To be conservative, therefore, we chose the same magnitude range $17.5 < m_r < 19.4$ and $17.5 < m_{r,\text{ec}} < 19.4$ for analysis, independent of the extinction correction; the dashed vertical lines in figure 3 indicate the above range for m_r , while the white regions correspond to that for $m_{r,\text{ec}}$, the extinction corrected magnitude.

The corresponding magnitude ranges in the other bands are similarly indicated in figure 3. In addition we checked that shifting the adopted magnitude ranges by up to 1 magnitude does not significantly affect our results.

The number of galaxies in the selected magnitude range (between the dashed lines) is on the order of 10^5 for the u -band and 10^6 for the other bands.

3. Analysis

3.1. Surface number density and average color of galaxies

We divide the entire selected survey region into 69 subregions grouped by their values of $A_{r,\text{SFD}}$. Each subregion consists of spatially separated (disjoint) small regions of the sky with $A_{r,\text{SFD}}$ values in a given interval. We define the intervals of $A_{r,\text{SFD}}$ such that the area of each subregion is approximately equal ($\sim 100 \text{ deg}^2$). The adopted intervals are shown by thin vertical lines in figure 2.

Figure 4 shows the surface number densities of galaxies, S_{gal} , for the 69 subregions as a function of its mean extinction value, $\bar{A}_{r,\text{SFD}}$. We define $\bar{A}_{r,\text{SFD}}$ simply by averaging $A_{r,\text{SFD}}$ for all galaxies located in the subregion. We select the r -band to represent the extinction simply because it is the central SDSS band and used for many selection cuts, and it is indeed trivial to translate the extinction to other bands using Table 6 of SFD.

The open circles indicate S_{gal} uncorrected for extinction, while the filled triangles indicate the results after the extinction correction. The crosses show the results using the extinction correction obtained from the galaxy number counts as explained in Section 3.2; all dependence of counts on extinction is removed by construction for the points plotted as crosses.

We compute an error estimate, ΔS , for S_{gal} in each subregion according to

$$(\Delta S)^2 = \frac{N}{\Omega^2} + \frac{N^2}{\Omega^3} \int_{\Omega} d\Omega' w(\theta'), \quad (2)$$

where N denotes the number of galaxies in the subregion with area Ω , and $w(\theta)$ is the angular correlation function of galaxies.

We adopt a double power-law model for $w(\theta)$:

$$w(\theta) = \begin{cases} 0.008(\theta/\text{deg})^{-0.75} & (\theta \leq 1\text{deg}) \\ 0.008(\theta/\text{deg})^{-2.1} & (\theta > 1\text{deg}) \end{cases}, \quad (3)$$

(Scranton et al. 2002; Fukugita et al. 2004).

Strictly speaking, the integral in equation (2) should be performed over the complex and disjoint shape of each subregion. However, for simplicity we adopt a circular approximation, integrating over $0 < \theta < \theta_c$ for the actual area of the subregion, i.e., out to $2\pi(1 - \cos\theta) = \Omega$. This approximation may slightly overestimate the true error, but it does not affect our conclusion. For the typical values of $N \sim 5 \times 10^4$ and $\Omega \sim 100 \text{deg}^2$, the second term is larger by two orders of magnitude than the first term. The above error-bars are plotted in figure 4.

Figure 4 indicates that the galaxy counts, uncorrected for extinction (open circles), decrease with increasing $\bar{A}_{r,\text{SFD}}$ for $\bar{A}_{r,\text{SFD}} > 0.1$, the expected effect of Galactic dust. However, the increase in galaxy counts with increasing extinction for $\bar{A}_{r,\text{SFD}} < 0.1$ is a surprise and is the opposite of the effect expected from Galactic dust. Furthermore, this puzzling feature remains even after the SFD extinction correction is applied (filled triangles). The SFD extinction correction does properly remove the expected anti-correlation of counts and extinction for $\bar{A}_{r,\text{SFD}} > 0.1$.

A presumably related anomaly can be also seen in the average color of galaxies against $\bar{A}_{r,\text{SFD}}$ for low extinctions. Figure 5 shows the average $g - r$ color of galaxies corresponding to figure 4. The color of galaxies before the extinction correction is redder at higher extinction for $\bar{A}_{r,\text{SFD}} > 0.1$, but is constant for $\bar{A}_{r,\text{SFD}} < 0.1$. After the SFD correction, the galaxy color is independent of $\bar{A}_{r,\text{SFD}}$ for $\bar{A}_{r,\text{SFD}} > 0.1$ as expected. Nevertheless the anti-correlation between $g - r$ and $\bar{A}_{r,\text{SFD}}$ is recognizable for $\bar{A}_{r,\text{SFD}} < 0.1$ (see inset in figure 5). A similar plot for $r - i$ color is shown in figure 6, but the above features are weak, though perhaps not entirely absent.

3.2. An additional extinction ΔC_x based on galaxy number counts

In order to investigate possible reasons for the anomalous behavior of galaxy counts at low SFD extinction, we derive an additional extinction correction ΔC_x , explicitly constructed to make the two quantities independent. In other words, by using the fact that S_{gal} should be independent of $A_{r,\text{SFD}}$ if the galaxy magnitudes are properly corrected for Galactic dust extinction, we solve for an additional extinction ΔC_x relative to $A_{x,\text{SFD}}$ that enforces this behavior.

Figure 7 shows the differential surface number density of galaxies, $dS/dm_{x,\text{ec}}$. Note that the magnitudes, $m_{x,\text{ec}}$, in this figure refer to the values corrected for the extinction using $A_{x,\text{SFD}}$. The black lines are the differential surface number density of galaxies in the entire survey region, $dS_e/dm_{x,\text{ec}}$. Those for each subregion, $dS/dm_{x,\text{ec}}$, are plotted in colored dots according to the value of $\bar{A}_{r,\text{SFD}}$ indicated in the color bar.

It is clear that low $A_{r,\text{SFD}}$ subregions (blue dots) preferentially lie below $dS_e/dm_{x,\text{ec}}$, while redder ones lie above it. This systematic trend is simply another representation of the anomalies

shown in figure 4. We now find the best fit values for the additional correction $\Delta C_x(\bar{A}_{x,\text{SFD}})$ by a χ^2 analysis for the shifted number density $dS/dm_{x,\text{ec}} - \Delta C_x$ in each subregion, and $dS_e/dm_{x,\text{ec}}$.

The results for ΔC_x as a function of $\bar{A}_{x,\text{SFD}}$ in the five different bands are plotted in figure 8. All the panels show the same systematic behavior for $A_{r,\text{SFD}} < 0.1$ which is required to cancel the anomaly in figure 4 (crosses). The S_{gal} with the additional correction is indeed completely independent of $\bar{A}_{r,\text{SFD}}$ within the quoted error-bars, which simply confirms that the calculation has been carried out correctly.

The same correction simultaneously removes the anomaly in the $g - r$ color of galaxies in figure 5 (crosses). This, however, is not a circular result and thus lends some credibility to the exercise since the same hypothetical additional dust component required to remove the anomaly in the counts need not also be one which eliminates the color anomaly.

Despite being internally self-consistent and simultaneously satisfying both count and color correction constraints with a single free function, the physical implications of this explanation of the anomalies, basically that they are due to an unknown component of Galactic dust, are not particularly plausible. In particular, the amplitudes of the corrections are surprisingly large, of order 0.1 to 0.2 magnitudes, and rather insensitive to the band in which they are defined (about half as large in z -band as in u -band). In the next section we subject the unknown dust component explanation to further tests and suggest an alternative and more plausible possibility.

4. Interpretation

In this section we will consider possible explanations for the surprising anomaly reported in the previous section, namely that there are fewer SDSS galaxies (in both raw and corrected counts) in regions of the sky where the SFD map indicates the least extinction, precisely the opposite of the trend one would naively expect.

4.1. Effects on counts of more distant objects

If the anomalous excess counts of SDSS galaxies at low values of $A_{x,\text{SFD}}$ reported above were actually due to systematic underestimation of the extinction at low extinction in the SFD map (*i.e.*, the most direct interpretation), then the same effect would also be apparent in the distribution of more distant cosmic objects. Here we show that this is not the case.

In order to see the extent to which the anomaly in S_{gal} depends on the distance of the sample, we repeat the same analysis separately for samples of nearby and more distant SDSS spectroscopic galaxies as well as for a SDSS photometric quasar sample (Richards et al. 2004). The results are summarized in figure 9. The different symbol colors indicate the surface number densities of photometric quasars (blue) and spectroscopic galaxies (red). The latter is further divided into two subsamples according to the redshift; $z > 0.1$ (green) and $z < 0.1$ (yellow). The open circles refer to the uncorrected data, while the filled ones to the data which are corrected

using $A_{x,\text{SFD}}$. Note that the selection criteria for the photometric quasar sample already make use of the SFD-extinction correction, but this should not invalidate our use of the data.

Clearly, the spectroscopic galaxy sample shows a similar anomaly at low $A_{r,\text{SFD}}$ to the one seen in the photometric galaxy sample. However, the effect is much weaker in the $z > 0.1$ subsample than in the $z < 0.1$ one. Moreover, the photometric quasar sample shows little, if any, sign of the effect at low extinction.

We find no obvious correlation between the $\bar{A}_{r,\text{SFD}}$ and the observed (uncorrected) mean surface density of QSO's for the cells in the range $\bar{A}_{r,\text{SFD}} < 0.15$. The galaxy clustering anomaly acts to shuffle cells in the $\bar{A}_{r,\text{SFD}} < 0.15$ range, producing spuriously higher and lower values of A_{SFD} around the level of any underlying galactic extinction. We expect that the anomaly is clustered like bright galaxies and therefore it should be unrelated to the surface density of distant QSO's. Hence, where we are dominated by this, we may expect a flatter relation between the QSO counts and A_{SFD} , as observed, washing out the weak underlying galactic extinction. A flat relation is also clear for the $z > 0.1$ galaxy sample, indicating they are in the background, relatively unrelated to the anomaly.

The fact that the SFD extinction corrected counts of distant objects are uncorrelated with the extinction while those of nearby objects exhibit the low $A_{x,\text{SFD}}$ anomaly strongly suggests that the effect is not solely a problem with the extinction map but must also be connected to the nearby galaxies as well. In order to further elucidate the situation, we now turn to an alternative indicator of Galactic extinction.

4.2. Galaxy surface number density versus an HI extinction map

We next investigate the correlation between the surface number density of SDSS photometric galaxies and the Leiden-Dwingeloo HI (21 cm) map (Hartmann & Burton 1997). The HI map can be used as a tracer of dust column density in optically thin regions. According to SFD, the conversion from the HI map to r -band extinction, $A_{r,\text{HI}}$, is given as follows.

$$\begin{aligned}
A_{r,\text{HI}} [\text{mag}] &= 2.751 \times 0.0184 [\text{mag}/(\text{MJy}/\text{sr})] \\
&\times 0.01222 [(\text{MJy}/\text{sr})/(\text{K km/s})] \\
&\times \sum_{-72 < v_{\text{LSR}} [\text{km/s}] < +25} 1.03 T_a(v_{\text{LSR}}) [\text{K km/s}],
\end{aligned} \tag{4}$$

where T_a is antenna temperature in the HI map. The 21 cm emission is summed up in the velocity range $-72 < v_{\text{LSR}} < +25$. *The velocity cut is very important because it rigorously excludes extragalactic effects on the Galactic extinction map.* In addition, it also removes the contribution of high velocity clouds which presumably have very little dust. Figure 10 shows the correlation between $A_{r,\text{HI}}$ and $A_{r,\text{SFD}}$. In the low extinction region ($A_{r,\text{SFD}} < 0.1$), the correlation is almost linear. Figure 11 shows the surface number density (no extinction correction) as a function of $A_{r,\text{HI}}$. In this figure, there is very little, if any, anomaly of the type seen in figure 4.

4.3. Likely Contamination of the SFD Extinction Map by Extragalactic FIR Emission

In attempting to understand the low extinction anomaly it is useful to keep in mind that $A_{x,\text{SFD}}$ is basically proportional to the $100\mu\text{m}$ flux observed in the IRAS/ISSA sky map, aside from modest dust temperature corrections derived from the COBE/DIRBE sky map at 100 and $240\mu\text{m}$. This means that the positive correlation between SDSS galaxy counts and $A_{x,\text{SFD}}$ can also be thought of as being a positive correlation with the $100\mu\text{m}$ flux. This suggests the obvious and plausible hypothesis that the correlation is simply due to the $100\mu\text{m}$ emission of the galaxies themselves, both those directly detected in the Sloan survey as well as other (optically) fainter ones which follow the galaxy clustering structures traced by the SDSS galaxies.

Figure 12 combines the information in Figures 10 and 11 and illustrates that the tight correlation of $\bar{A}_{r,\text{SFD}}$ and $\bar{A}_{r,\text{HI}}$ extends to very small extinctions. More importantly, we note that $\bar{A}_{r,\text{SFD}}$ is slightly but systematically larger for larger S_{gal} , which is clearly exhibited in the lower panel. On the other hand, the weak departure from linearity below 0.02 is an artifact due to the averaging procedure over bins of $\bar{A}_{r,\text{HI}}$ with the presence of noises; we made sure that the data points shift to the right, instead of downward, when the average is taken over the bins of $\bar{A}_{r,\text{SFD}}$.

This again suggests that the galaxy count behavior in the low A_{SFD} regions is related to some effect in the construction of the SFD map and not to some previously unknown component of Galactic dust.

The hypothesis can be most clearly understood by examining the shape of the relationship between raw galaxy counts and $A_{x,\text{SFD}}$ shown by the red points in figure 4. At SFD extinctions above the peak in S_{gal} in each band, we suppose that the observed $100\mu\text{m}$ flux is indeed dominated by Galactic dust emission and thus that the inferred SFD extinction is thus a good indicator of the actual extinction; as expected the raw galaxy counts then fall with increasing extinction. However, at SFD extinctions below this peak, we suppose that extragalactic FIR emission is making a substantial, perhaps dominant, contribution to the total $100\mu\text{m}$ flux and thus producing the observed positive correlation between galaxy counts and SFD inferred extinction. In other words, we can still observe the intrinsic correlation of extragalactic optical and FIR emission where the Galactic dust emission is weak enough to unveil it.

Of course, SFD were aware of the possibility of extragalactic contributions to the observed IRAS/ISSA $100\mu\text{m}$ flux and attempted to minimize it by both subtracting the contributions of approximately 10,000 known point sources from the sky map and then subtracting a uniform flux density of $\nu I_\nu \sim 25 \text{ nWm}^{-2}\text{sr}^{-1}$ at $100\mu\text{m}$ in order to remove the *mean* contribution of fainter, unresolved point sources. However, it is clear that neither procedure can remove the *fluctuations* in the background extragalactic FIR light due to faint sources. It is these fluctuations, interpreted as variations in Galactic extinction in the SFD map, which we believe to be responsible for the observed anomaly.

We may now investigate this hypothesis quantitatively by comparing the extinction

inferred from galaxy number counts (as in section 3.2) with that inferred from $100\mu m$ flux by SFD on the assumption that there is actually a contribution to this flux from galaxies at the expected level.

First we note that Finkbeiner, Davis & Schlegel (2000) detected the infrared background at a level of $\nu I_\nu \sim 25 \text{ nWm}^{-2}\text{sr}^{-1}$ at $100\mu m$. This corresponds to about 0.015 mag in $E(B - V)$, (~ 0.04 mag in A_r). This value is comparable to the $A_{r,\text{SFD}}$ values in the region where the anomalous positive correlation of surface number density of galaxies exist with $A_{r,\text{SFD}}$ is observed. By itself this indicates that the order-of-magnitude strength of the hypothesized contamination is appropriate to explain the anomaly.

Second if fluctuations in galaxy surface density on the sky are attributed entirely to dust, the ratio of the observed surface number density in a certain direction, S_{gal} and the average of the surface number density of galaxies over the whole sky, \bar{S}_{gal} can be written as

$$S_{x,\text{gal}}/\bar{S}_{x,\text{gal}} = 10^{-\gamma_x \Delta C_x}, \quad (5)$$

where γ_x and ΔC_x are the slope of dS/dm_x and the correction to the $A_{x,\text{SFD}}$ required to yield uniform galaxy counts across the sky (see section 3.2), respectively. On the other hand, if *fluctuations* in galaxy surface density on the sky comes from the contamination of total FIR flux by extragalactic flux, the expected correction to the $A_{x,\text{SFD}}$, $\Delta A_{x,\text{IR}}$ can be written as

$$\Delta A_{x,\text{IR}} = k_{x/r} \frac{0.04}{\bar{S}_{x,\text{gal}}} (\bar{S}_{x,\text{gal}} - S_{x,\text{gal}}), \quad (6)$$

where $k_{x/r}$ is the conversion factor from A_r to A_x . Therefore, the relation between ΔC_x and $\Delta A_{x,\text{IR}}$ is

$$\Delta A_{x,\text{IR}} = 0.04 k_{x/r} (1 - 10^{-\gamma_x \Delta C_x}). \quad (7)$$

Note that equations (5) to (7) should be interpreted as an order-of-magnitude relation, but illustrate the qualitative effect of the IR emission of galaxies on the estimate of the *Galactic* extinction. Figure 13 shows $\Delta A_{x,\text{IR}}$ converted by equation (7) from ΔC_x which is shown in figure 8. *Thus the amplitude of $\Delta A_{x,\text{IR}}$ is about one-tenth that of ΔC_x .* This quantitative analysis supports the extragalactic FIR contamination hypothesis. It shows that rather small systematic errors, of order hundredths of a magnitude, in the SFD extinction values (at low extinction) can plausibly explain the surprisingly large values of ΔC_x shown in figure 8.

Note that one cannot use the above relationship directly as a correction to A_{SFD} because it only applies on average (over 100 deg^2 regions of the sky) but would not improve the extinction estimate for individual pixels in the SFD map. In principle, some combination of the observed SDSS galaxy counts in each SFD pixel and the observed $100\mu m$ flux could be combined to provide an improved estimate of the actual extinction; however, in practice this is not likely to be very successful due to the Poisson noise in the SDSS map at the SFD angular resolution (corresponding to only of order a single survey galaxy per pixel). Moreover, the absolute correction to the SFD extinction would be quite small, of order 0.01-0.02 magnitudes,

although the relative correction could be substantial on the sight-lines with already very low SFD extinctions.

As a final test of the hypothesis, we simulate the expected effect using mock data and show that it is consistent with the observations. We constructed a mock galaxy sample with the Poisson noise in the same region of the sky as the SDSS survey area, and counted the mock galaxies in pixels as defined in SFD map (each pixel has 5.635 min^2 area). Then we use the existing SFD-map as the “true” dust extinction and add extra “extinction”, inferred from the assumed extra $100\mu\text{m}$ flux, proportional to the number of galaxies in each pixel according to

$$A_{r,c} = A_{r,\text{SFD}} + c_r(N_{\text{mock}} - \bar{N}_{\text{mock}}), \quad (8)$$

where $A_{r,c}$ is the calculated r -band model extinction when the extragalactic FIR flux is not distinguished from the infrared emission from Galactic dust. Thus c_r and N_{mock} are the mean conversion factor and number of mock galaxies in a pixel. We then computed the “observed” surface number density of mock galaxies, $S_{\text{mock,obs}}$, as follows:

$$S_{\text{mock,obs}} = S_{\text{mock}} 10^{(-0.5A_{r,c})}, \quad (9)$$

where S_{mock} is the true surface number density of mock galaxies. The open square and open triangle in figure 14 show S_{mock} and $S_{\text{mock,obs}}$, respectively. It exhibits the same qualitative behavior seen in figure 4 and is even more dramatic due to the absence of all noise and measurement errors.

5. Summary

We have compared the SFD Galactic extinction map to the number counts of SDSS photometric galaxies. For SFD extinctions above 0.1 to 0.2 magnitudes, depending on the band, we find the two types of estimates to be in tolerable agreement on average. However, for smaller values of the SFD extinction, we find a substantial and systematic disagreement. In particular, we find that that average galaxy counts (surface density on the sky) *increase* and average galaxy colors become slightly *redder* with *increasing* SFD extinction, precisely the opposite of expected dust effects. This low SFD extinction regime exhibiting anomalous behavior includes approximately 68% of the high Galactic latitude sky covered by the SDSS, as well as most other observations of extragalactic objects.

Although one could explain the observations with a hypothetical component of Galactic dust which is somehow anti-correlated the $100\mu\text{m}$ flux based SFD-map, this does not seem physically plausible. In addition there is no sign of such a component in HI based extinction maps. Moreover, the surface number density of distant quasars does not exhibit any such anomaly, as would be expected if it arose from some unknown component of Galactic dust. Therefore, we conclude the effect is not due to major deficiencies in the SFD extinction map.

An alternative and more reasonable explanation is provided by the hypothesis that residual FIR emission from external galaxies contaminates the signal from Galactic dust and becomes

the dominant contribution on sight-lines where the actual Galactic extinction and, thus, dust emission are low. We show that this explanation is quantitatively plausible and consistent with the observed effect. An extragalactic FIR flux corresponding to only of order 0.01 magnitudes of inferred SFD extinction is sufficient to explain the anomaly. Moreover, simulation of the effect with mock data reproduces the anomaly’s major qualitative and quantitative features.

Assuming the above interpretation to be correct, our results represent good news in one respect and bad news in another:

In the former sense, it is reassuring that the implied systematic errors in the widely used SFD extinction map are quite small in magnitude, of order hundredths of a magnitude, and in the range those authors expected; in other words, they are not likely to be a significant problem for most applications.

However, the bad news is that these systematic errors are themselves correlated with the spatial clustering and distribution of galaxies in some complex and potentially pernicious way. For “precision cosmology” applications that depend sensitively on the accuracy of statistical measures of galaxy clustering (*e.g.*, the power spectrum or baryon acoustic oscillations), it will be necessary to disentangle the signal from a systematic source of noise (the extinction) which depends on the signal one is trying to measure (Yahata et al. 2005; Eisenstein et al. 2005). Moreover, studies of galaxy clustering are ordinarily carried out in regions of the sky selected to have low extinction, *i.e.*, just those in which the systematic extinction errors are most strongly correlated with the large scale structure. We plan to address this and related problems in future work.

We thank Naoki Yasuda and J. Mohr for useful discussions. K. Y. was supported by Grants-in-Aid for Japan Society for the Promotion of Science Fellows. ELT’s participation in the project was supported in part by NASA grant NAG5-13148.

Funding for the SDSS and SDSS-II has been provided by the Alfred P. Sloan Foundation, the Participating Institutions, the National Science Foundation, the U.S. Department of Energy, the National Aeronautics and Space Administration, the Japanese Monbukagakusho, the Max Planck Society, and the Higher Education Funding Council for England. The SDSS Web Site is <http://www.sdss.org/>.

The SDSS is managed by the Astrophysical Research Consortium for the Participating Institutions. The Participating Institutions are the American Museum of Natural History, Astrophysical Institute Potsdam, University of Basel, Cambridge University, Case Western Reserve University, University of Chicago, Drexel University, Fermilab, the Institute for Advanced Study, the Japan Participation Group, Johns Hopkins University, the Joint Institute for Nuclear Astrophysics, the Kavli Institute for Particle Astrophysics and Cosmology, the Korean Scientist Group, the Chinese Academy of Sciences (LAMOST), Los Alamos National Laboratory, the Max-Planck-Institute for Astronomy (MPIA), the Max-Planck-

Institute for Astrophysics (MPA), New Mexico State University, Ohio State University, University of Pittsburgh, University of Portsmouth, Princeton University, the United States Naval Observatory, and the University of Washington.

References

- Abazajian, K. et al. 2003 AJ, 126, 2081
Abazajian, K. et al. 2004 AJ, 128, 502
Adelman-McCarthy, J. K., et al. 2006 ApJS, 162, 38
Blanton, M. R., Lin, H., Lupton, R. H., Maley, F. M., Young, N., Zehavi, I., & Loveday, J. 2003, AJ, 125, 2276
Burstein, D. & Heiles, C. 1978 ApJ, 225, 40
Burstein, D. & Heiles, C. 1982 AJ, 87, 1165
Cardelli, J., A., Clayton, G., C. & Mathis, J., S. 1989 ApJ, 345, 245
Connolly, A., J. et al. 2002 ApJ, 579, 42
Eisenstein et al. 2005, ApJ, 633, 560
Faber, S. M., Wegner, G., Burstein, D., Davies, R. L., Dressler, A., Lynden-Bell, D. & Terlevich, R. J. 1989, ApJS, 69, 763
Fukugita, M., Ichikawa, T., Gunn, J. E., Doi, M., Shimasaku, K., & Schneider, D. P. 1996 AJ, 111, 1748
Fukugita, M., Yasuda, N., Brinkmann, J., Gunn, J. E., Ivezić, Ž., Knapp, G. R., Lupton, R. & Schneider, D. P. 2004 AJ, 127, 3155
Finkbeiner, D., P., Davis, M. & Schlegel, D. 2000 ApJ, 544, 81
Gunn, J. E., et al. 1998, AJ, 116, 3040
Gunn, J. E., et al. 2006, AJ, 131, 2332
Hogg, D. W., Finkbeiner, D. P., Schlegel, D. J., & Gunn, J. E. 2001, AJ, 122, 2129
Kennicutt, R. C. 1998 ARA&A, 36, 189
Hartmann, D. & Burton, W. B. 1997 Atlas of Galactic Neutral Hydrogen (Cambridge : Cambridge Univ. Press)
Ivezić, Ž., et al. 2004, AN, 325, 583
Maddox, S., J., Efsthathiou, G. & Sutherland, W. J. 1996 MNRAS, 283, 1227
Pier, J. R., Munn, J. A., Hindsley, R. B., Hennessy, G. S., Kent, S. M., Lupton, R. H., & Ivezić, Ž. 2003, AJ, 125, 1559
Richards, G. T., et al. 2004 ApJS, 155, 257
Schlegel, D., Finkbeiner, D., & Davis, M. 1998 AJ, 500, 525
Scranton, R. et al. 2002 ApJ, 579, 48
Smith, J. A., et al. 2002, AJ, 123, 2121
Stoughton, C., et al. 2002 AJ, 123, 485
Strauss, M. et al. 2002 AJ, 124, 1810
Tucker, D., et al. 2006, AN, in Press

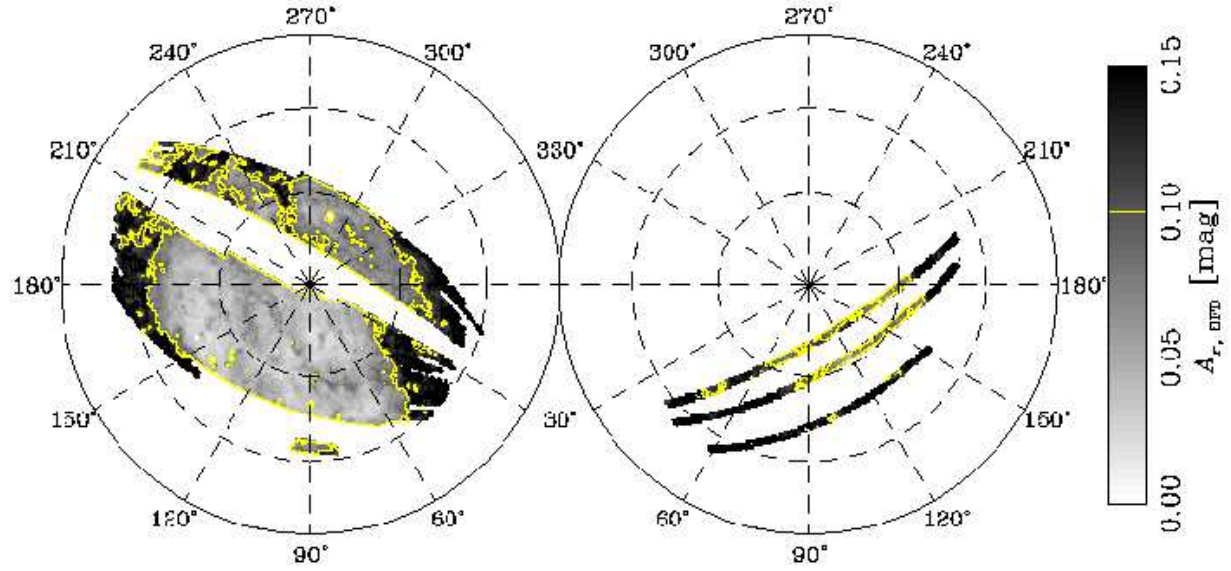


Fig. 1. Photometric survey area of the SDSS DR4 in Galactic coordinates. The gray scale indicates the magnitude of $A_{r,SFD}$, as indicated by at the right. The region in which $A_{r,SFD} < 0.1$ is indicated by a contour line.

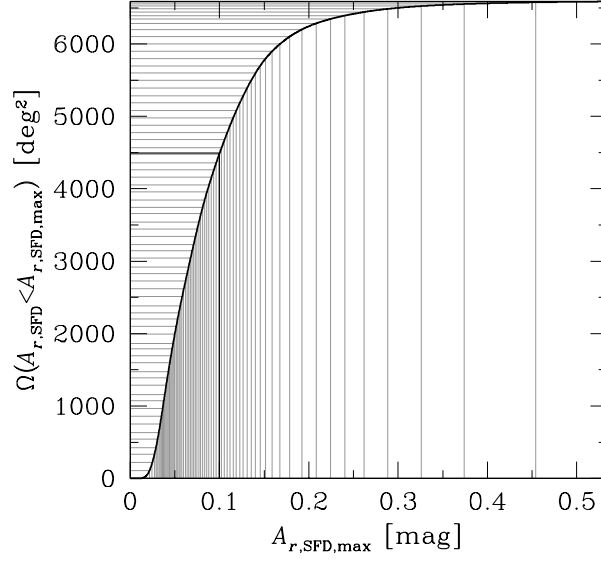


Fig. 2. Cumulative distribution of sky area as a function of $A_{r,\text{SFD},\text{max}}$. Note that $A_{r,\text{SFD}}$ is less than 0.1 mag for the majority of the survey region, approximately 68% in fact, as denoted by the heavy vertical and horizontal lines. The vertical gray lines show the division of the SDSS survey region (see section 3.1) according to extinction values. The horizontal gray lines indicate the corresponding area.

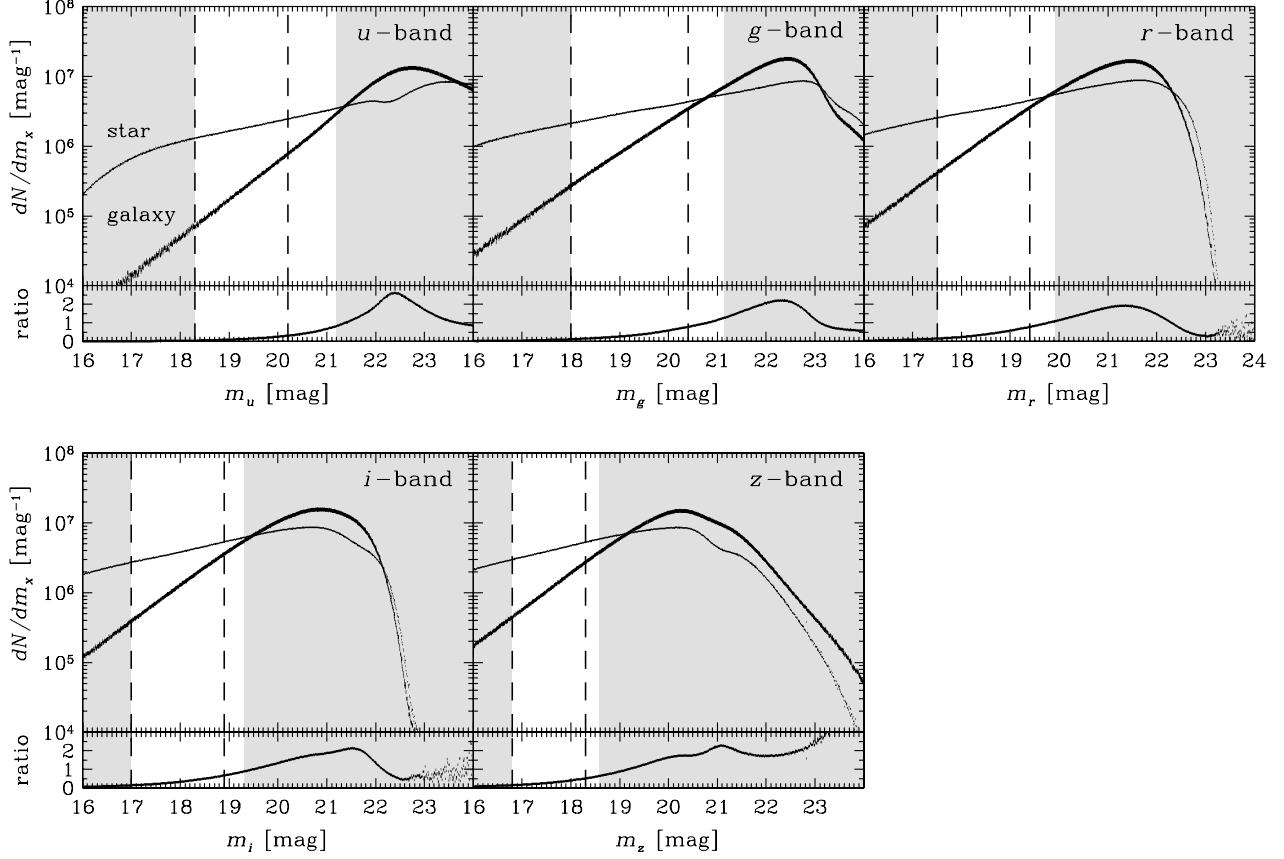


Fig. 3. Differential number counts of galaxies (thick line) and stars (thin line) (*upper part of each panel*), and the number ratio of galaxies to stars (*lower part of each panel*) as a function of magnitude (no extinction correction). The two vertical dashed lines show the magnitude range in which we compute the surface number density of galaxies. The upper left, the upper middle, the upper right, the lower left and the lower right panels correspond to data for u -, g -, r -, i - and z -bands, respectively. In the r -band, we choose the magnitude range $17.5 < m_r < 19.4$ (the dashed vertical lines in the *upper right panel*). Even for the extinction corrected magnitude $m_{r,ec}$, we choose the same magnitude range which is plotted as a white region. The range of analysis differs from band to band, and they are similarly indicated in the other panels.

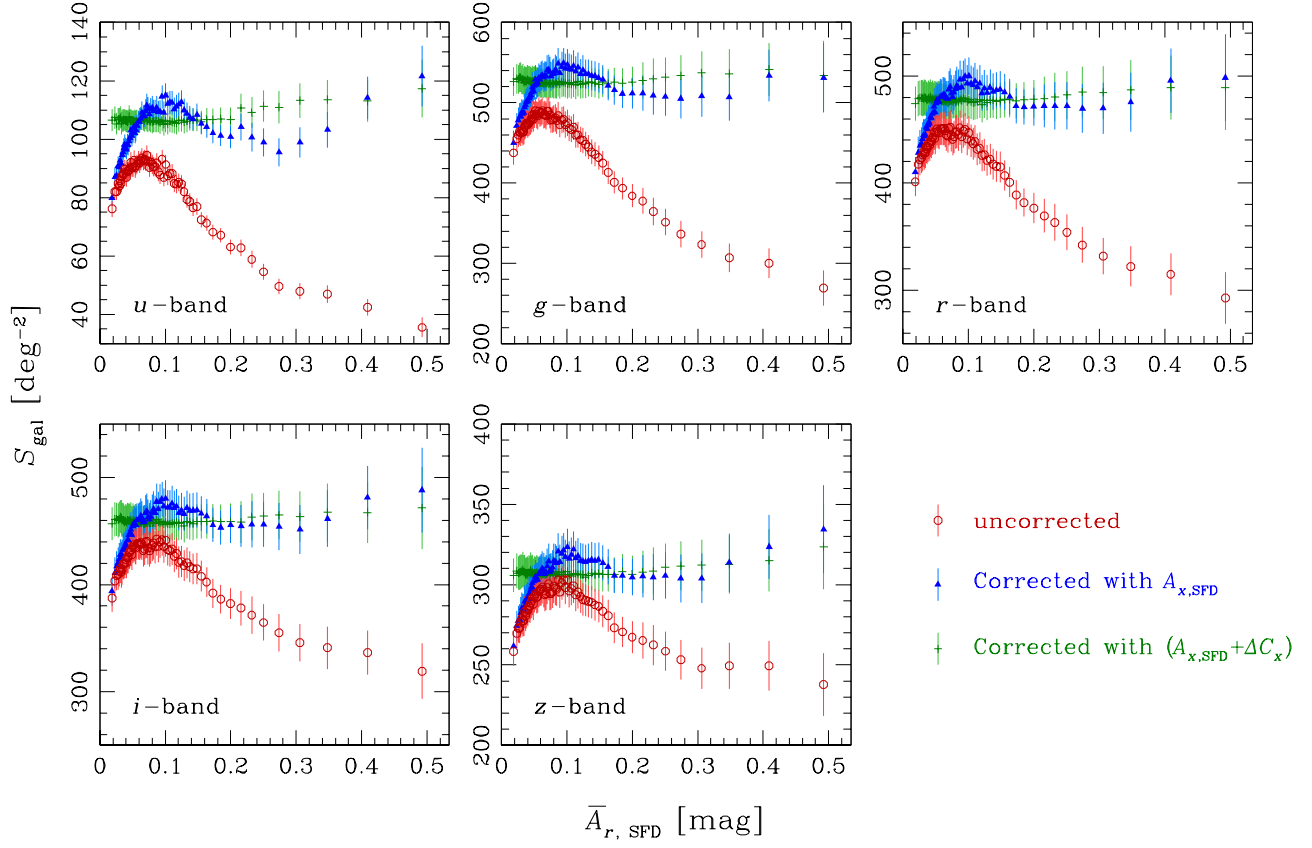


Fig. 4. Surface number density of SDSS DR4 photometric sample galaxies in each subregion. The horizontal axis is the mean SFD-extinction for the subregion, $\bar{A}_{r, \text{SFD}}$. The open circles (filled triangles) indicate that the magnitude is corrected (not corrected) using $A_{x, \text{SFD}}$. The crosses indicate the magnitude after an additional extinction derived from the galaxy counts (see section 3.2). The error bars are calculated using eq. 2.

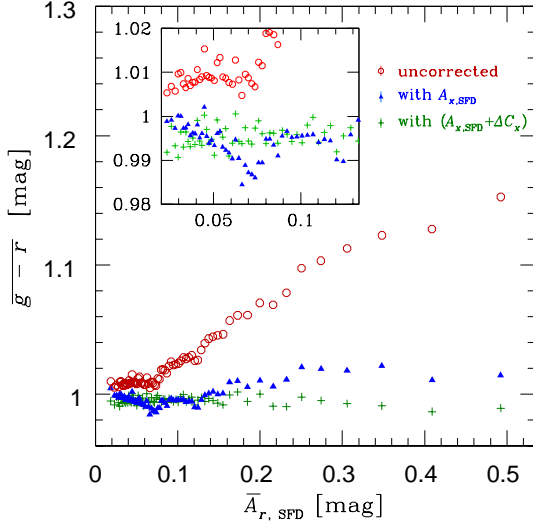


Fig. 5. The average $g - r$ color of galaxies in each subregion as a function of $A_{r,\text{SFD}}$. The symbols are also the same as in figure 4.

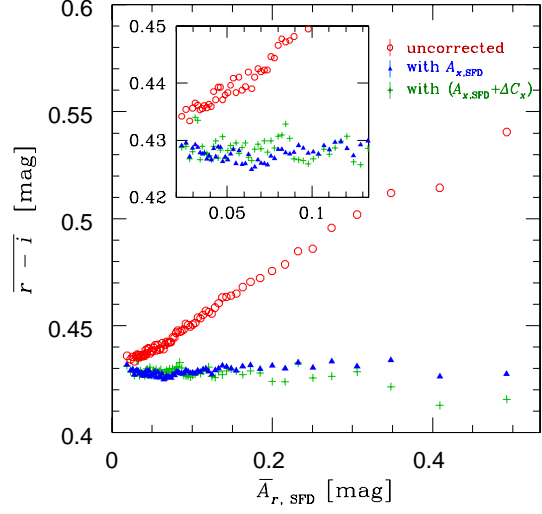


Fig. 6. Same as figure 5 but for average $r - i$ color.

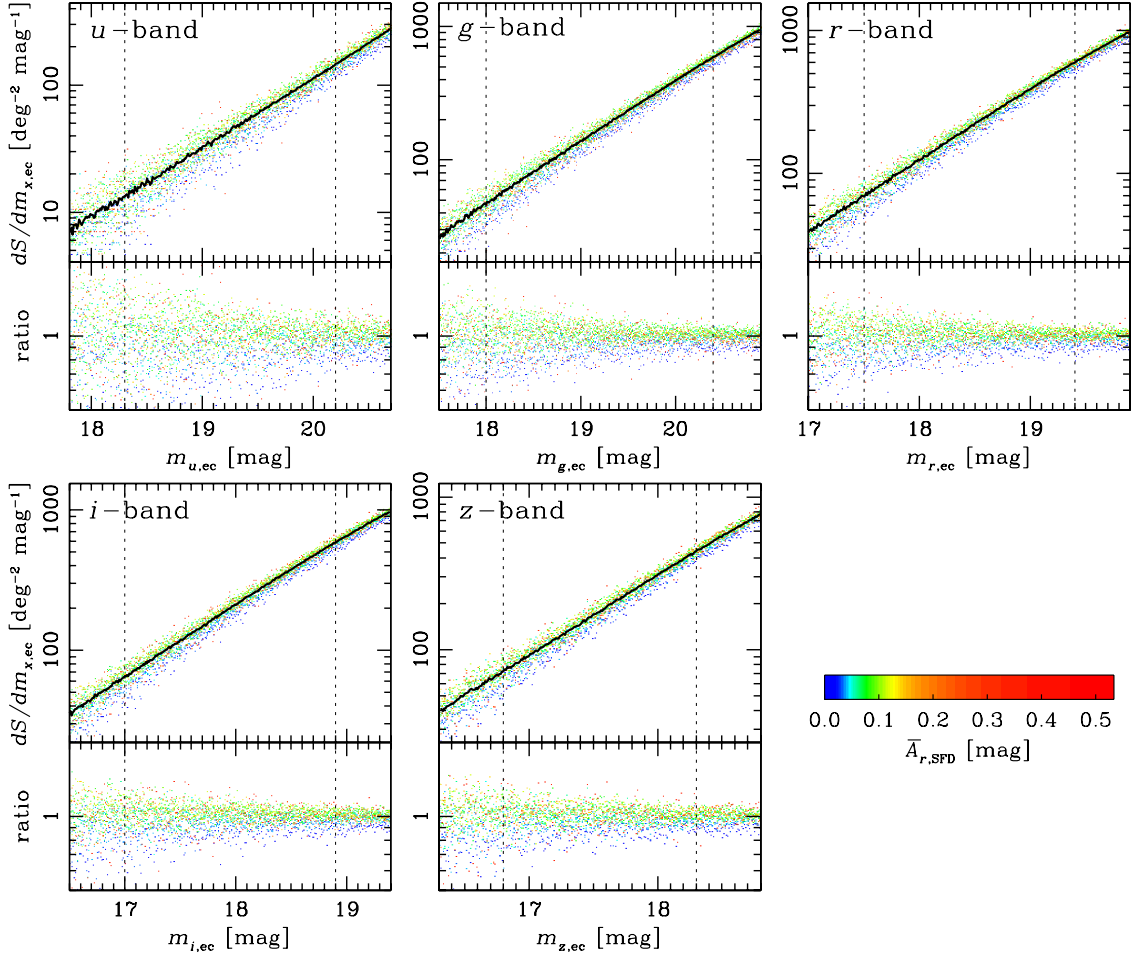


Fig. 7. Differential surface number density of galaxies, $dS/dm_{x,\text{ec}}$ for subregions (colored dots) and $dS_e/m_{x,\text{ec}}$ (black dots) (*upper part of each panel*), and the ratio of $dS/dm_{x,\text{ec}}$ to $dS_e/m_{x,\text{ec}}$ (*lower part of each panel*). The bluer dots correspond to data for low A_{SFD} regions and redder lines correspond to those for high A_{SFD} regions. The two vertical dashed lines are the same as those in figure 3. The observational band for each panel is the same as in figure 3.

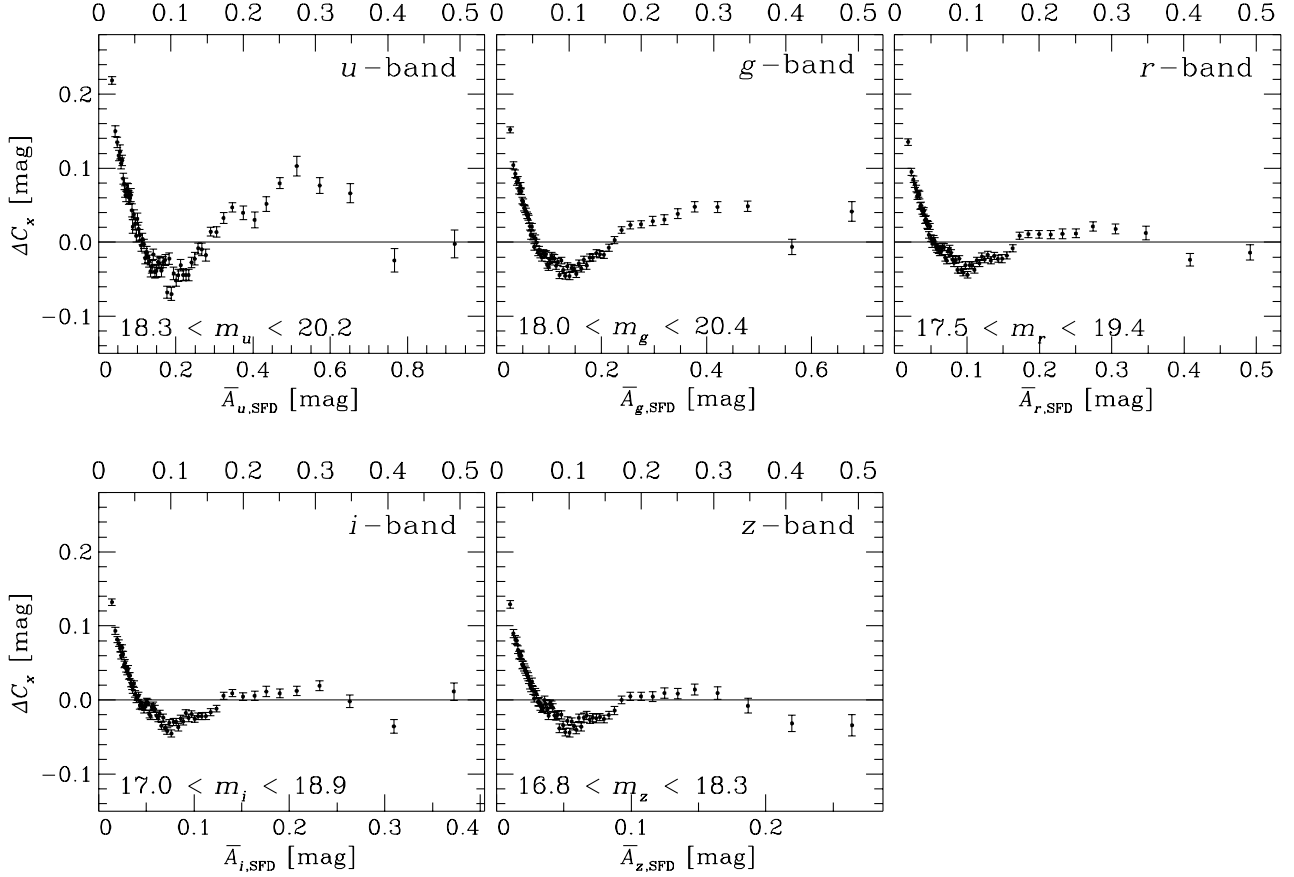


Fig. 8. The additional extinction ΔC_x required to give a constant corrected galaxy surface number density in each subregion. The horizontal axis is the mean $A_{x,\text{SFD}}$ in each band and is scaled so that the relative positions of a subregion in each of the five panels are the same (the upper scales indicate the corresponding $A_{r,\text{SFD}}$ values). Error bars are evaluated by the χ^2 minimization procedure to fit $dS/dm_{x,\text{ec}} - \Delta C_x$ to $dS_e/dm_{x,\text{ec}}$.

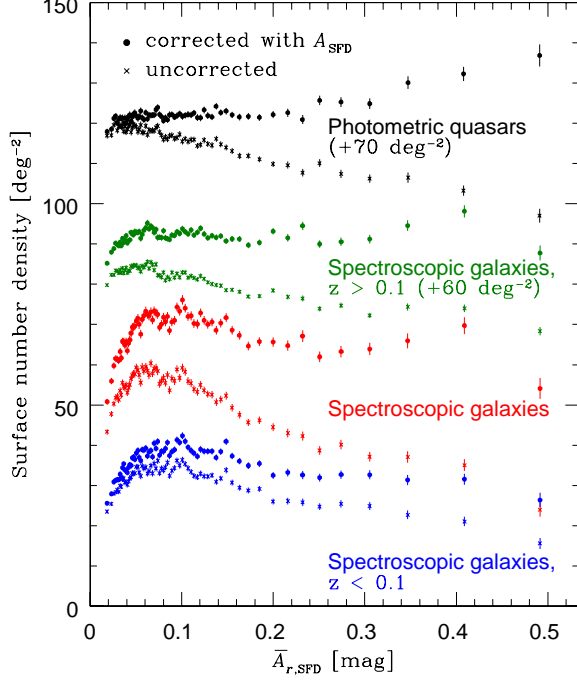


Fig. 9. Surface number density of SDSS photometric quasars and spectroscopic galaxies as a function of $\bar{A}_{r,\text{SFD}}$. The filled circles and the crosses indicate the results with and without an extinction correction using $A_{x,\text{SFD}}$, respectively. Just for clarity, the data points of photometric quasars and spectroscopic galaxies with $z > 0.1$ are shifted upward by $+70\text{deg}^{-2}$ and $+60\text{deg}^{-2}$, respectively. The error bars are $1\text{-}\sigma$ Poisson error.

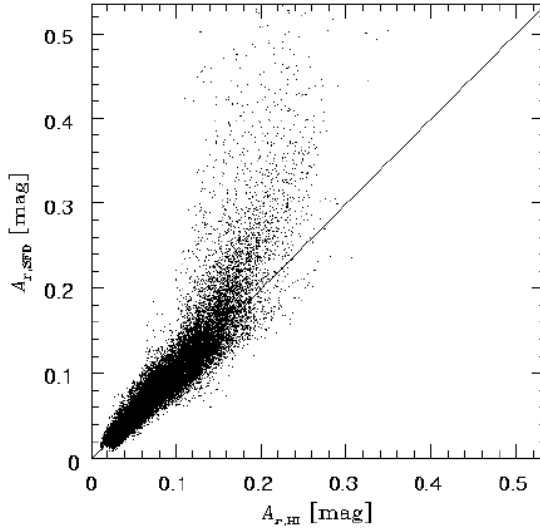


Fig. 10. Correlation between $A_{r,\text{SFD}}$ and $A_{r,\text{HI}}$. The latter is estimated from the Leiden-Dwingeloo HI (21 cm) map (Hartmann & Burton 1997).

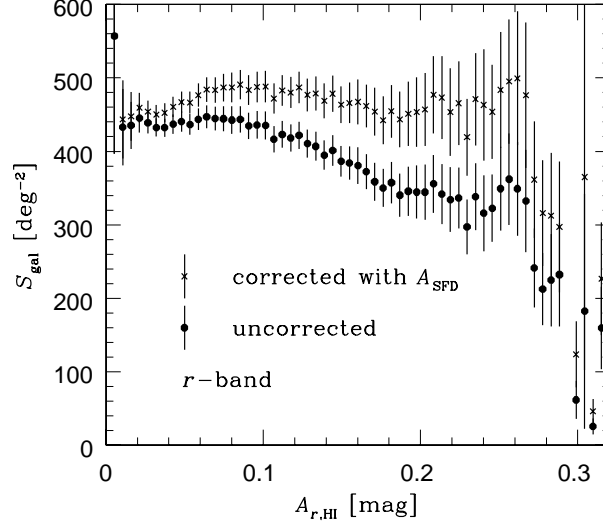


Fig. 11. Surface number density of galaxies as a function of $A_{r,\text{HI}}$. Filled circles and crosses indicate S_{gal} before and after correcting for the extinction using $A_{r,\text{SFD}}$, respectively.

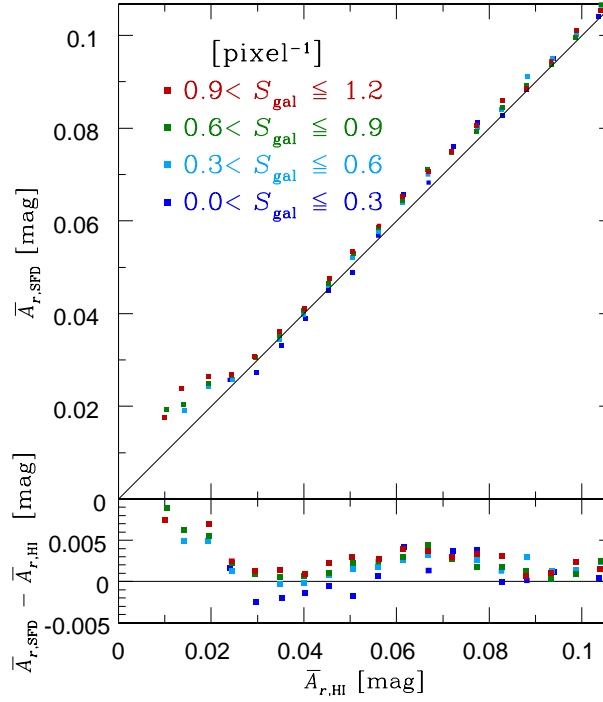


Fig. 12. Correlation between $A_{r,\text{SFD}}$ and $A_{r,\text{HI}}$ binned according to S_{gal} .

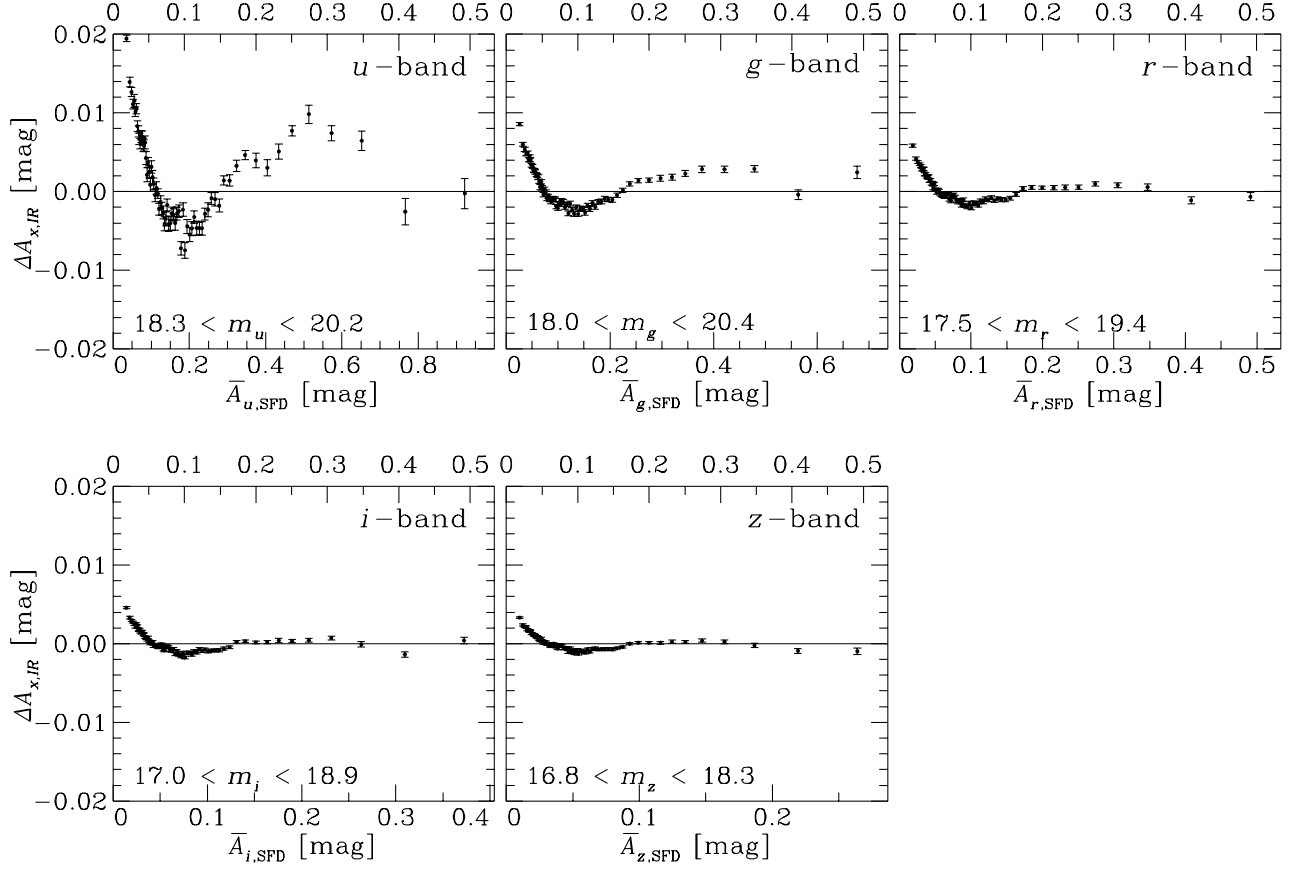


Fig. 13. The mean correction $\Delta A_{x,IR}$ to $A_{x,SFD}$ implied by the hypothesis of extragalactic FIR contamination of the SFD-map. The vertical axis is the mean extinction in the SFD-map which is actually due to this contamination rather than actual Galactic dust (see eq.[7]).

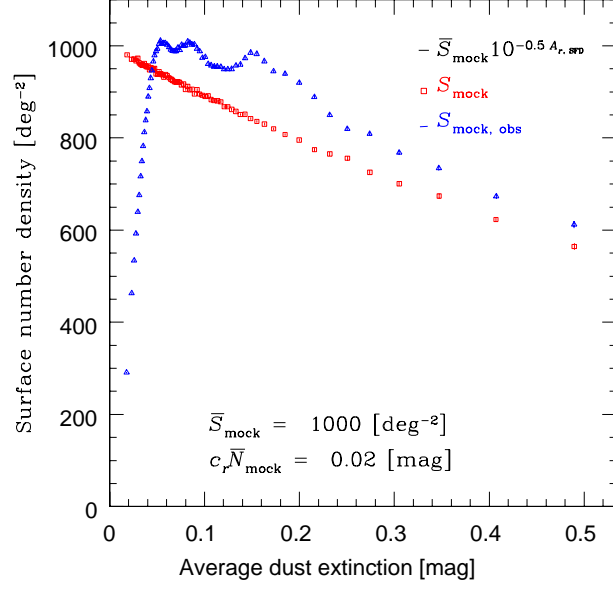


Fig. 14. Simulated surface number density of galaxies in a mock survey as a function of $\bar{A}_{r,c}$ or $\bar{A}_{r,\text{SFD}}$. The open triangle (square) corresponds to extragalactic FIR emission contamination (or absence thereof) of the FIR Galactic dust emission. We set the surface number density of mock galaxies, \bar{S}_{mock} , to 1000 deg^{-2} and the typical contribution to the $A_{r,\text{SFD}}$ of those galaxies, $c_r \bar{N}_{\text{mock}}$, to 0.02 mag .